Analytical Biochemistry 410 (2011) 92–97

Contents lists available at ScienceDirect

Analytical Biochemistry

journal homepage: www.elsevier.com/locate/yabio

Noncovalent functionalization of carbon nanotubes with lectin for label-free dynamic monitoring of cell-surface glycan expression

Yadong Xue, Lei Bao, Xirui Xiao, Lin Ding, Jianping Lei, Huangxian Ju *

Key Laboratory of Analytical Chemistry for Life Science (Ministry of Education of China), Department of Chemistry, Nanjing University, Nanjing 210093, People's Republic of China

ARTICLE INFO

Article history:
Received 9 August 2010
Received in revised form 3 November 2010
Accepted 11 November 2010
Available online 19 November 2010

Keywords:
Cytosensing
Electrochemistry
Carbon nanotubes
Cell-surface glycan
Carbohydrates
Lectin

ABSTRACT

A kind of concanavalin A functionalized multiwalled carbon nanotube (ConA-MWCNT) was constructed by noncovalent assembly of ConA on carboxylated MWCNT with poly(diallyldimethylammonium) as a linker. The novel nanomaterial was characterized with scanning electron microscopy and atomic force microscopy. It incorporated both the specific recognition ability of lectin for cell-surface mannosyl groups and the unique electronic and mechanical properties of MWCNT. An electrochemical label-free method for cytosensing was proposed by constructing a ConA-MWCNT interface on a glassy carbon electrode, which showed a linear response to K562 cells ranging from 1×10^4 to 1×10^7 cells mL^{-1}. The ConA-MWCNT interface could be further used for monitoring of dynamic variation of glycan expression on K562 cells in response to drugs. A facile and high-throughput optical method for the analysis of dynamic glycan expression on living cells was also developed by constructing an array of ConA-MWCNT spots on a glass slide. This method showed acceptable rapidity and low cost. The noncovalent functionalization of MWCNTs with lectins could be potentially applied in cell biological studies based on cell-surface glycan expression.

The functionalization of carbon nanotubes (CNTs)[1] can extremely extend their application in affinity separations, biosensing, bioreactors, and the construction of biofuel cells [1–4]. Therefore, much effort has been devoted to finding cost-effective approaches to functionalize CNTs by attachment of biomolecules [5–10] , which can generally be immobilized on CNTs by two approaches: covalent binding [11,12] and noncovalent attachment [6,13,14]. Covalent binding usually needs some cross-linker agents, and the activity of the immobilized biomolecules may be affected due to the steric hindrance by covalent binding [15]. Furthermore, a covalent approach may cause a partial loss of the electronic properties of functionalized CNTs [16]. On the contrary, the physical adsorption and electrostatic binding used in noncovalent attachment can maintain the activity of biomolecules on the CNTs. In view of the advantages of noncovalent attachment, our previous work focused on functionalized multiwalled carbon nanotubes (MWCNTs) with arginine–glycine–aspartic acid–serine peptide for cell capture [12,17]. This work further constructed a kind of concanavalin A (ConA) functionalized multiwalled carbon nanotube (ConA-MWCNT) on both electrode surfaces and glass slides, and developed two methods for label-free analysis of dynamic glycan expression on living cells.

Glycans account for a large degree of cell-surface structural variations, and form complicated codes for cellular physiology [18–21]. Dynamic change in the glycosylation status on carcinoma cell surfaces has been considered to play important roles in oncogenic transformation, cell differentiation, and metastasis [22,23]. Thus, it is urgent to develop sensitive, practical, and high-throughput monitoring technology for analyzing these changes and further providing diagnostic tools to guide treatment. Several electrochemical methods based on the specific recognition of lectins have been developed for sensitive monitoring of dynamic change in the glycosylation status [17,24]. Compared with conventional mass spectrometry [25–27] and lectin microarray approaches [28–30], these methods can obviate cell lysis, cell labeling, or complicated instrumentation. However, most of the electrochemical methods use nanoparticles or enzymes to label the recognition element lectins, which may disturb the biological activity of lectins, and the complexity and laboriousness are typically increased for a tagging protocol. Although a label-free strategy has been developed for electrochemical analysis of cell-surface glycans by covalently immobilizing lectins on single-walled carbon nanohorns [31], the covalent binding was complicated and time-consuming.

In this work, the noncovalent functionalization of MWCNTs with ConA was proposed by using poly(diallyldimethylammonium) (PDDA) as a linker. Owing to the ConA isoelectric point of

* Corresponding author. Fax: +86 25 83593593.
E-mail address: hxju@nju.edu.cn (H. Ju).

[1] *Abbreviations used*: BSA, bovine serum albumin; CNTs, carbon nanotubes; ConA, concanavalin A; MWCNTs, multiwalled carbon nanotubes; PBS, phosphate-buffered saline; PDDA, poly(diallyldimethylammonium).

0003-2697/$ - see front matter © 2010 Elsevier Inc. All rights reserved.
doi:10.1016/j.ab.2010.11.019

4.5–5.5 [32], PDDA and ConA could be integrated sequentially onto carboxylic group-functionalized MWCNTs at pH 7.4, as shown in Fig. 1. The successful assembly of uniform and stable ConA-MWCNT membranes on both electrode and glass surfaces was demonstrated using scanning electron microscopic (SEM), atomic force microscopic (AFM), and contact angle techniques. Based on the ConA-MWCNT membranes, an electrochemical label-free strategy and an array of ConA-MWCNT spots were presented for specific monitoring of dynamic variation of glycan expression on K562 cells in response to drug (Fig. 1). The array allowed a facile optical high-throughput analysis of cell-surface glycans. Both the electrochemical and optical methods could obviate the destruction or labeling of cells and the covalent tagging of lectin, and thus could be potentially applied in cell biological studies based on cell-surface glycan expression.

Materials and methods

Chemicals and materials

ConA, PDDA (20%, w/w in water, MW: 200,000–350,000), and bovine serum albumin (BSA) were purchased from Sigma-Aldrich, Inc. (USA). Mannose (Man) and *N*-acetylglucosamine (GlcNAc) of analytical grade were from Sinopharm Chemical Reagent Co., Ltd (China). Swainsonine (SW) was from Merck KGaA (Darmstadt, Germany). Fluorescein lectin kit I containing fluorescein isothiocyanate (FITC)-labeled ConA was purchased from Vector Laboratories, Inc. (USA). Fluorescein (FITC)-labeled mannose was obtained from Sigma-Aldrich, Inc. MWCNTs (CVD method, purity $\geqslant$98%, diameter 20–40 nm, and length 1–2 μm) were purchased from Nanoport Co., Ltd. (Shenzhen, China). Phosphate-buffered saline (PBS, pH 7.4) containing 136.7 mM NaCl, 2.7 mM KCl, 87 mM Na_2HPO_4, and 14 mM KH_2PO_4 was sterilized before use. Other reagents were of analytical grade. All aqueous solutions were prepared using $\geqslant$18 MΩ ultrapure water purified with a Millipore Milli-Q system.

Apparatus

Electrochemical impedance spectroscopic (EIS) measurements were performed on a PGSTAT30/FRA2 system (Autolab, Netherlands) in 0.01 M, pH 7.4, PBS containing 5 mM $K_4Fe(CN)_6$, 5 mM $K_3Fe(CN)_6$, and 0.1 M KCl using a conventional three-electrode system with modified GCE as working, platinum wire as auxiliary, and saturated calomel electrode as reference electrodes. The impedance spectra were recorded within the frequency range of 5×10^{-2}–10^5 Hz, and the amplitude of the applied sine wave potential was 5 mV. Flow cytometry was carried out on a FACS Calibur flow cytometer (Becton Dickinson, USA). SEM and AFM images were observed under a Hitachi S-4800 scanning electron microscope (Japan) and an Agilent 5500 atomic force microscope (USA), respectively. Bright-field images of cells were taken by a TE2000-U inverted fluorescence microscope (Nikon, Japan). The static water contact angles were measured at 20 °C by a contact angle meter (Rame-Hart-100) employing drops of pure deionized water.

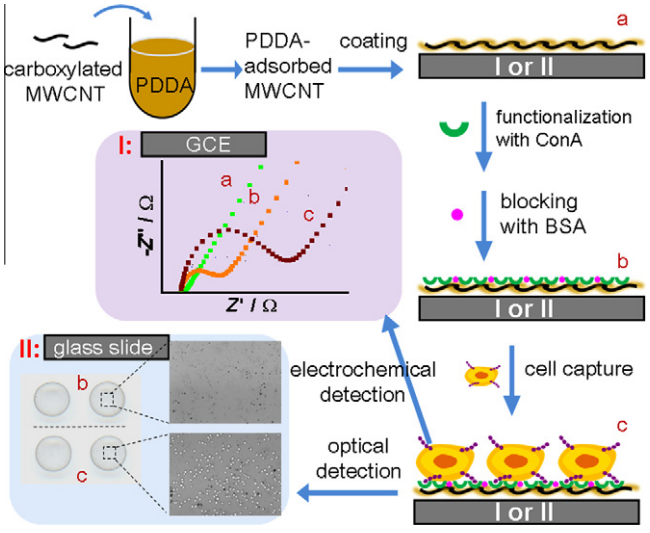

Fig.1. Scheme of noncovalent lectin functionalization of MWCNTs and electrochemical (I) and optical (II) monitoring of dynamic glycan expression on living cells.

Cell line and cell culture

The K562 cell line was kindly provided by the Affiliated Zhongda Hospital, Southeast University, Nanjing, China. K562 cells were cultured in a flask in RPMI 1640 medium (GIBCO) supplemented with 10% fetal calf serum (Sigma), penicillin (100 μg mL^{-1}), and streptomycin (100 μg mL^{-1}) at 37 °C in a humidified atmosphere containing 5% CO_2. After culture for 72 h, the cells were collected and separated from the medium by centrifugation at 1000 rpm for 10 min, and then washed thrice with a sterile, pH 7.4, PBS. The sediment was resuspended in PBS to obtain a homogeneous cell suspension. Cell number was determined using a Petroff–Hausser cell counter (USA). SW-treated K562 cells were obtained by incubating the cells in a culture medium containing 2 μg mL^{-1} SW for different times [33].

Preparation of PDDA-functionalized MWCNTs

MWCNTs were first treated with 3/1 H_2SO_4/HNO_3 in sonication for 4 h. The resulting dispersion solution was filtered and washed repeatedly with water until pH was about 7.0. This procedure shortened MWCNTs, removed metallic and carbonaceous impurities, and generated carboxylate groups on the surface. Next, the carboxylated MWCNTs of 0.5 mg mL^{-1} were dispersed into a 0.2% PDDA aqueous solution by a 30-min sonication to give a homogeneous black solution. Residual PDDA polymer was removed by high-speed centrifugation, and the complex was thrice washed with water to obtain PDDA-functionalized MWCNTs.

Cytosensor preparation

GCE was first polished with 1.0, 0.3, and 0.05 μm α-Al_2O_3 powder (Beuhler) successively. After sonication in water, the electrode was rinsed with deionized water and allowed to dry at room temperature. PDDA-functionalized MWCNT solution (5 μL, 0.5 mg mL^{-1}) was dropped on the pretreated GCE and dried in a desiccator to obtain PDDA-MWCNT/GCE, which was then immersed in 5 μL PBS containing optimal concentrations of lectin for 20 min to yield ConA-MWCNT/GCE. Following a slight rinse with 0.01 M, pH 7.4, PBS, the modified electrode was soaked in PBS containing 1% BSA for 20 min to block the surface. A 5 μL K562 cell suspension at a certain concentration containing 1 mM Ca^{2+} and Mn^{2+} was dropped on the lectin-immobilized electrode and incubated at 25 °C for 50 min. Here Ca^{2+} and Mn^{2+} were used for maintaining the binding activity of ConA to cell-surface mannosyl groups. After carefully rinsing with PBS to remove the noncaptured cells, the obtained electrode was ready for impedance measurement.

Construction of ConA-MWCNT array on a glass slide

A glass slide was first dipped in ethanol for 1 h to clean the surface. After being washed thoroughly with water, it was dried under a stream of nitrogen. Four drops of PDDA-MWCNT solution (0.5 μL, 0.5 mg mL^{-1}) were transferred onto the pretreated glass slide to form a 2 × 2 array and allowed to dry, which produced four stable PDDA-MWCNT spots. Then, 0.5 μL, pH 7.4, PBS containing optimal concentration of lectin was dropped onto each spot and incubated for 20 min to yield ConA-MWCNT/glass. Following BSA blocking for 20 min and rinsing with PBS, 5 μL K562 cell suspension containing 1 mM Ca^{2+} and Mn^{2+} was dropped on each spot and incubated in a humidified atmosphere at 25 °C for 50 min. After slightly rinsing with PBS to remove noncaptured cells, the obtained cells/ConA-MWCNT/glass array was ready for optical measurement with the fixed time of exposure. The trypan blue staining experiment showed that 95% of the captured cells kept good viability.

Cell counting for optical analysis

The cell counting procedure was similar to the reported approach for lectin arrays [34]. After being imaged by an inverted microscopy, the density of the captured cells on ConA-MWCNT spot was counted by reading the relative gray scale intensity (*I*) using Adobe Photoshop software [35]. Briefly, each optical image was first converted to a black image with the color level of (0, 0.1, 255). Then, the *I* value of each image was recorded for analysis, which represented the mean shades of gray. A larger number of captured cells corresponded to a higher *I*.

Monosaccharide inhibition assay

The ConA-MWCNT/glass was preincubated with 5 μL 200 mM monosaccharide (Man or GlcNAc) dissolved in PBS for 50 min at 25 °C [36]. After carefully rinsing with PBS, 5 μL K562 cell suspension at 1.0×10^6 cells mL^{-1} was dropped onto the preincubated ConA-MWCNT/glass and incubated for 50 min in a humidified atmosphere at 25 °C. After slightly rinsing with PBS to remove the noncaptured cells, the obtained glass slide was used for optical investigation.

Flow cytometric analysis

Untreated and SW-treated K562 cells were collected and separated from the medium by centrifugation at 200*g* at room temperature for 6 min. Subsequently, the cells were washed with sterile cold PBS, and resuspended in PBS. The cell concentration was determined. Then, 50 μL of 1×10^7 cells mL^{-1} cell suspension and 445 μL of PBS were mixed with 5 μL of 1 mg mL^{-1} FITC-labeled ConA, and incubated at room temperature for 30 min. The cells were collected by centrifugation at 200*g* for 6 min, washed twice with 200 μL cold PBS, resuspended in 500 μL of PBS, and assayed by flow cytometry. Fluorescent intensity (FI) of unlabeled K562 cells was used for estimation of autofluorescence.

Results and discussion

Characterization of noncovalently ConA-functionalized MWCNTs

Cationic polyelectrolyte PDDA can wrap on the sidewall surface of the carboxylated MWCNTs for loading of negatively charged enzymes by a layer-by-layer assembly [7]. In this work, the positively charged PDDA-modified carboxylated MWCNTs were employed for the electrostatic adsorption of negatively charged ConA for the specific recognition of cell-surface glycans. The SEM image of PDDA-MWCNT film showed a homogeneous surface and good dispersion with the outer diameter ranging from 25 to 45 nm (Fig. 2A). This uniform and interdigitated nanostructure provided a significant increase of effective area for lectin loading. The noncovalent ConA-MWCNT film also displayed a well-dispersed three-dimensional structure (Fig. 2C), but the diameter distribution increased by 10 nm, suggesting the densely packed lectin on the surface of MWCNTs. SEM images at higher magnification indicated the obvious morphological change between PDDA-MWCNTs and ConA-MWCNTs (Fig. 2B and D). The latter surface appeared plump in texture and the aggregation of lectin was also observed on the cross section of MWCNTs.

AFM as a useful tool for surface imaging was also employed for the characterization of functionalized MWCNTs. Tapping mode AFM images of isolated PDDA-MWCNT and ConA-MWCNT are shown in Fig. 2E and F. Size analysis showed that the MWCNT after PDDA adsorption had an average height of 35 nm, whereas the MWCNT with lectin attached had an average height of 45 nm. The 10-nm increase in height for ConA-MWCNT was consistent with the SEM results. Furthermore, after lectin loading, globular shapes suggestive of protein aggregates appeared on the side wall of the nanotube [9]. Both SEM and AFM images verified the successful functionalization of MWCNTs by ConA through the noncovalent approach. Fluorescent microscopic images of the functionalized MWCNTs further demonstrated the uniform functionalization (Supplementary Fig. S1). After incubation with FITC-labeled mannose the ConA-functionalized MWCNTs showed clear green fluorescence with even distribution, while the MWCNTs did not show any fluorescence signal, indicating no binding site

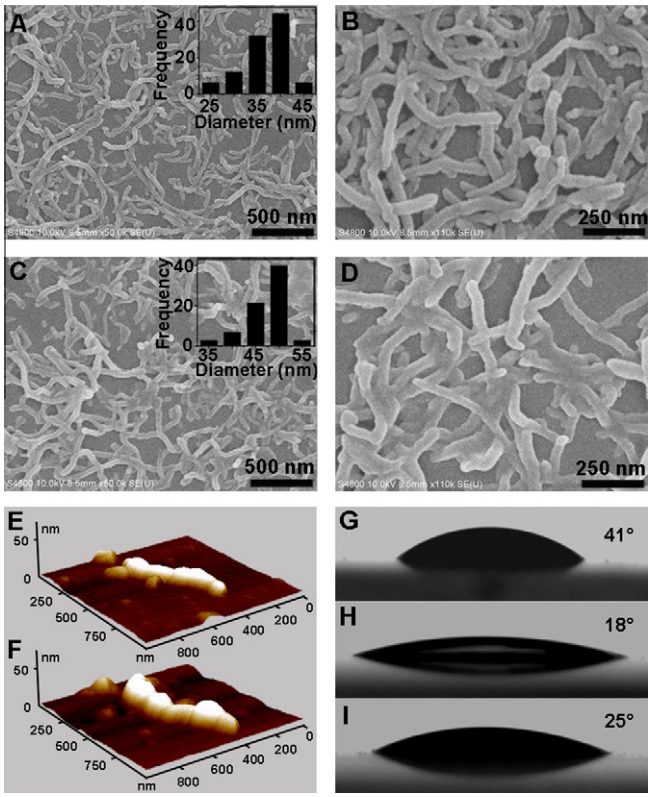

Fig.2. SEM images of (A,B) PDDA-MWCNT and (C,D) ConA-MWCNT films, tapping mode AFM images of (E) PDDA-MWCNT and (F) ConA-MWCNT isolated on mica surface, and contact angles of (G) bare, (H) PDDA-MWCNT, and (I) ConA-MWCNT-modified substrates. Inset: diameter distributions of (A) PDDA-MWNTs and (C) ConA-MWCNTs.

of FITC-labeled mannose on the surface of MWCNTs, and the uniform attachment of ConA on the functionalized MWCNT surface.

The uniform structure of ConA-MWCNT film facilitated the accessibility of cells to lectins and resulted in improved sensitivity for cytosensing.

The biocompatibility of an interface can be characterized by its hydrophilicity, which can be qualitative by measuring the contact angle of the substrate [6]. The contact angles of the bare glass slide, PDDA-MWCNT, and ConA-MWCNT film were measured to be 41°, 18°, and 25°, respectively (Figs. 2G–I). The lower contact angle of PDDA-MWNT film than that of the glass slide indicated better hydrophilicity due to more hydrophilic groups, which were produced on MWCNTs by acidic treatment. The improved biocompatibility of PDDA-MWNTs could preserve the bioactivity of the immobilized lectins.

Electrochemical cytosensing based on noncovalent ConA-MWCNTs

As schemed in Fig. 1, the assembly approach allowed the construction of three-dimensional noncovalent ConA-MWCNT recognition interface on a GCE surface by layer-by-layer assembly. The obtained uniform ConA-MWCNT film could capture K562 cells effectively via membrane mannosyl groups, owing to the specific recognition ability of lectin to cell-surface glycans [37]. The binding extent of K562 cells to the surface of ConA-MWCNT/GCE was evaluated by monitoring the change of electron-transfer resistance (R_{et}) at electrode surface using $[Fe(CN)_6]^{3-/4-}$ as redox probes (Fig. 3A). The bare GCE showed a low resistance (curve a in Fig. 3A), and the successive assembly of the PDDA-MWCNT layer on the electrode surface significantly facilitated the interfacial electron transfer (curve b in Fig. 3A). After ConA attachment and subsequent BSA blocking, the electron transfer resistance increased (curve c in Fig. 3A). Evidently, lectin acted as an inert electron- and mass-transfer blocking layer. The binding of K562 cells through specific interaction between membrane glycans and the corresponding lectin immobilized on GCE further hindered the access of the redox probes to the electrode, leading to a high R_{et} value (curve d in Fig. 3A). The increase in the magnitude of R_{et} (ΔR_{et}) correlated with the number of cells specifically bound to the electrode, which depended on the number of binding sites on cells captured by ConA-MWCNT/GCE, and thus reflected the amount of target glycan expressed on the cell surface. The MWCNTs increased both the surface area for cell recognition and the electrical connectivity, thus improving the detection sensitivity.

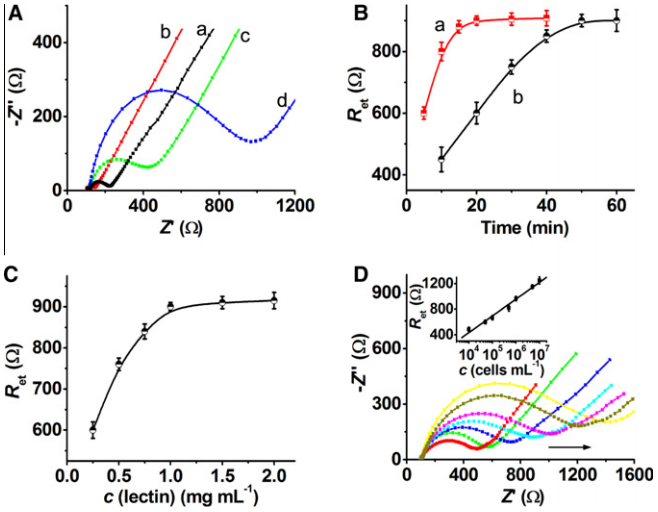

Fig.3. (A) Electrochemical impedance spectra of (a) GCE, (b) PDDA-MWCNT/GCE, (c) ConA-MWCNT/GCE, and (d) K562 cells/ConA-MWCNT/GCE in pH 7.4 PBS containing 0.1 M KCl, 5 mM $K_4Fe(CN)_6$, and 5 mM $K_3Fe(CN)_6$. (B) Plots of electron-transfer resistance (R_{et}) at (d) vs. incubation time for (a) ConA adsorption and (b) cell capture. (C) Plot of R_{et} at (d) vs. ConA concentration. (D) Electrochemical impedance spectra of (d) obtained with 1.0×10^4, 5.0×10^4, 1.0×10^5, 5.0×10^5, 1.0×10^6, 5.0×10^6, and 1.0×10^7 cells mL^{-1} K562 cells (from left to right). Inset: linear calibration curve.

The binding time for electrostatic adsorption between PDDA-MWCNTs and ConA was important for the loading of lectins onto MWCNTs, which further affected the cell-capture extent (curve a in Fig. 3B). After incubation with 5 μL of 1×10^6 cells mL^{-1} K562 cells, the R_{et} value obtained at resulting K562 cells/ConA-MWCNT/GCE increased with the increasing adsorption time, and tended to a constant value at 20 min, indicative of the maximum loading of lectins. The recognition time was also an important parameter for the kinetic binding between lectins and cell-surface glycans [17]. Thus, the R_{et} values at ConA-MWCNT/GCE after incubation with K562 cells for different times were investigated (curve b in Fig. 3B). With the increasing recognition time, R_{et} increased and tended to a constant value at 50 min, suggesting the saturated capture of K562 cells at ConA-MWCNT/GCE surface. Therefore, 20 and 50 min were chosen as the optimal times for electrostatic adsorption of lectin and specific capture of cells, respectively. Significantly, the proposed noncovalent approach was much faster than the covalent approach which required more than 3 h for the immobilization of lectins [31].

For the maximum capture of K562 cells at the ConA-MWCNT/GCE surface, the initial ConA concentration was also optimized (Fig. 3C). The optimal concentration of lectin was 1 mg mL^{-1}, at which the impedance response at K562 cells/ConA-MWCNT/GCE was related to the cell concentration used. The EIS curves at ConA-MWCNT/GCE after incubation with K562 cells of different concentrations for 50 min (Fig. 3D) indicated that the impedance response increased with the increasing cell concentrations, giving a linear relationship between the R_{et} value and the logarithmic value of the cell concentration ranging from 1.0×10^4 to 1.0×10^7 cells mL^{-1} with a correlation coefficient R of 0.992 ($n = 5$) (inset in Fig. 3D). Considering the fact that the volume of K562 cell suspension for incubation step was only 5 μL, the designed label-free strategy could detect the cell suspension containing as few as 50 individual K562 cells. The low detection limit was attributed to the high efficiency of the noncovalent functionalization of MWCNTs with ConA. Although the detection limit was higher than that based on reverse transcriptase PCR technology for cancer study [38], it was worth noting that the ConA-MWCNT-based label-free strategy avoided cell lysis and cell labeling, thus was very convenient and facile.

Specific capture of K562 cells by ConA-MWCNTs and cell-surface glycan

To validate the specificity of the interaction between cell-surface glycan and ConA-MWCNTs, a monosaccharide inhibition assay was performed on a glass slide combined with optical observation (Fig. 4). After incubation with 1.0×10^6 cells mL^{-1} K562 cell suspension, the PDDA-MWCNT/glass did not show any cells (Fig. 4A), while a uniform distribution of K562 cells was observed on the surface of ConA-MWCNT/glass (Fig. 4B), suggesting the ability of ConA-MWCNTs for effective capture of cells. On the Man-preincubated ConA-MWCNT/glass after incubation with K562 cells, the active sites of ConA for mannosyl groups were blocked, thus greatly inhibited the ability for cell capture (Fig. 4C). However, when GlcNAc was used as the blocking molecule, the attached ConA on the interface did not recognize GlcNAc, and the cell-capture extent was almost not influenced (Fig. 4D). The monosaccharide inhibition experiment demonstrated that the ability of ConA-MWCNTs to effectively capture cells was attributed to the

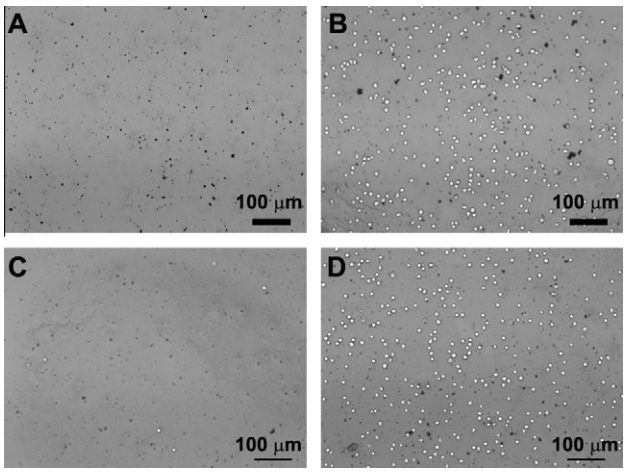

Fig.4. Optical micrographs of (A) PDDA-MWCNT/glass, (B) ConA-MWCNT/glass, (C) Man- and (D) GlcNAc-preincubated ConA-MWCNT/glass after incubation with 1.0×10^6 cells mL^{-1} K562 cells for 50 min.

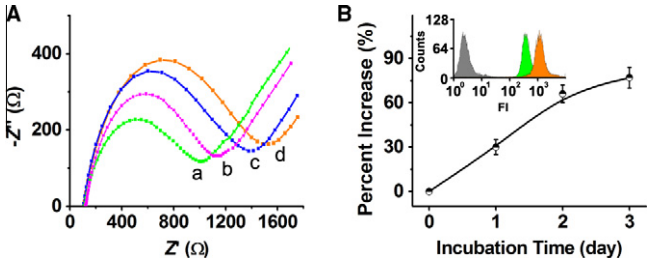

Fig.5. (A) Electrochemical impedance spectra of K562 cells/ConA-MWCNT/GCE obtained with K562 cells treated with SW for (a) 0, (b) 1, (c) 2, and (d) 3 days, and (B) effect of SW-treated time on electron-transfer resistance (R_{et}). The percentage increase is calculated with $[T/C - 1] \times 100\%$, where T and C are the ΔR_{et} at ConA-MWCNT/GCE on capture of SW-treated and untreated K562 cells, respectively. Inset: flow cytometric analysis of mannose moieties on untreated K562cells (green) and K562 cells treated with SW for 3 days (orange) with fluorescein-labeled Con A, and autofluorescence of unlabeled K562 cells (gray). FI: fluorescent intensity.

specific interaction between the immobilized lectins and cell-surface mannosyl groups. Thus, the lectin-MWCNTs were further applied for the label-free monitoring of dynamic glycan expression on living cells via electrochemical and optical strategies, respectively.

Electrochemical label-free monitoring of dynamic cell-surface glycan expression

The ConA-MWCNT-based strategy allowed its application in monitoring of the dynamic alteration of glycan expression on living cells in response to drug, using SW as a model. SW, a specific mannosidase II inhibitor [33], could increase the expression of terminal high-mannose-type glycan on the cell surface. During treatment with SW over 3 days, EIS curves at ConA-MWCNT/GCE after incubation with SW-treated K562 cells displayed an increasing impedance response compared with untreated cells (Fig. 5A). Because the ΔR_{et} correlated with the number of cells specifically bound to the electrode, which depended on the number of binding sites on cells, the increased ΔR_{et} reflected the progressively increased amount of target glycan expressed on the cell surface in response to SW treatment. Using untreated K562 cells as a control, the time-dependent percentage increase of ΔR_{et} on cell binding is shown in Fig. 5B, giving a statistically significant day-to-day change ($P < 0.05$, calculated by one-way ANOVA) [28]. To validate the observed change, the SW-treated K562 cells were stained with FITC-conjugated ConA and assayed using flow cytometry (inset in Fig. 5B), which also showed an increased binding to FITC-ConA compared with untreated K562 cells. These results indicated the increase of terminal mannose groups on the cell surface and the modification effect of SW on cell-surface glycosylation, demonstrating that the ConA-MWCNT-based electrochemical strategy could be used for sensitive monitoring of the dynamic alteration of glycan expression on living cells.

Optical label-free investigation of dynamic cell-surface glycan expression

As shown in Fig. 6A, an array of uniform ConA-MWCNT spots could be easily constructed on the glass slide by a similar layer-by-layer assembly. The obtained well-shaped, transparent spots could also capture K562 cells specifically via cell-surface mannosyl groups, leading to a facile label-free optical strategy for the high-throughput analysis of dynamic cell-surface glycan expression (Fig. 1). After incubation with SW-treated K562 cells, bright-field images showed that the cell-capture extent varied along with the treatment time of drug (Fig. 6B). During treatment with SW over 3 days, a growing distribution of captured cells could be observed. Further analysis of the numbers of captured cells by reading the relative gray scale intensity of each image revealed clearly the time-dependent effect of SW on the cell-capture extent (Fig. 6C), suggesting the progressively increased amount of target glycan expressed on the cell surfaces, which was consistent with the results of electrochemical measurement. Compared with the covalently fabricated lectin array on a gold substrate for optical profiling cell-surface glycan expression [34,39], the noncovalent approach combined with a glass slide was simple and low-cost, and preserved the bioactivity of the immobilized lectins. The lectin-MWCNT/glass array-based optical strategy allowed rapid and high-throughput profiling of cell-surface glycans expression by increasing the number of lectins present in the array.

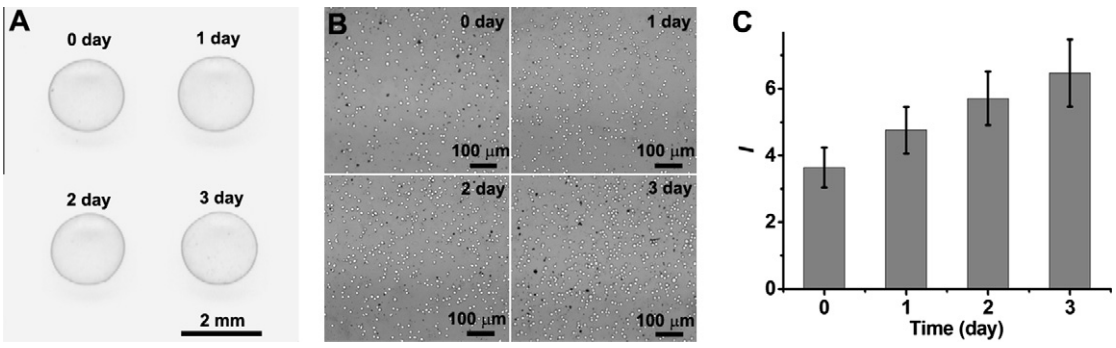

Fig.6. (A) Photo of a 2×2 array of ConA-MWCNT/glass spots and (B) bright-field images of each spot center after incubation with different SW-treated K562 cells, and (C) plot of relative gray scale intensity vs. SW-treated time.

Reproducibility and stability of ConA-MWCNT-based assay

At cell concentrations of 1.0×10^4 and 1.0×10^7 cells mL^{-1}, the R_{et} measured for six times at K562 cells/ConA-MWCNT/GCE showed the relative standard deviations of 4.8% and 6.2%, respectively, showing good reproducibility. When stored in 0.01 M, pH 7.4, PBS at 4 °C, no obvious change in the response to K562 cells was observed after 1 week of storage. This implied that the electrostatic interaction was very stable and the proposed noncovalent strategy was efficient for retaining the bioactivity of lectin.

Conclusions

This work constructed noncovalently lectin-functionalized MWCNTs. The uniform lectin-MWCNTs incorporated both the specific recognition ability of lectin for cell-surface glycan and the unique electronic and mechanical properties of MWCNTs. Based on the ability of lectin-MWCNTs to specifically capture cells, two facile label-free electrochemical and optical strategies were developed for the monitoring of dynamic glycan expression on living cells in response to drug. The electrochemical strategy showed good analytical performance, while the array-based optical strategy allowed the low-cost, rapid, and high-throughput analysis of cell-surface glycans. These strategies obviated the destruction or labeling of cells and the covalent tagging of lectin, thus providing a promising platform for profiling cell-surface glycan expression and would potentially contribute to meeting the challenges in unraveling the complex mechanisms underlying biological processes related to glycans.

Acknowledgments

We gratefully acknowledge the National Science Funds for Creative Research Groups (20821063), the Major Research Plan (90713015), and General Program (20875044) from the National Natural Science Foundation of China, and National Basic Research Program of China (2010CB732400).

Appendix A. Supplementary data

Supplementary data associated with this article can be found, in the online version, at doi:10.1016/j.ab.2010.11.019.

References

[1] W.R. Yang, K.R. Ratinac, S.P. Ringer, P. Thordarson, J.J. Gooding, F. Braet, Carbon nanomaterials in biosensors: should you use nanotubes or grapheme, Angew. Chem. Int. Ed. 49 (2010) 2114–2138.
[2] K. Balasubramanian, M. Burghard, Chemically functionalized carbon nanotubes, Small 1 (2005) 180–192.
[3] H. Chen, C. Yu, C. Jiang, S. Zhang, B. Liu, J. Kong, A novel near-infrared protein assay based on the dissolution and aggregation of aptamer-wrapped single-walled carbon nanotubes, Chem. Commun. (2009) 5006–5008.
[4] J. Ryu, H.-S. Kim, H.T. Hahn, D. Lashmore, Carbon nanotubes with platinum nano-islands as glucose biofuel cell electrodes, Biosens. Bioelectron. 25 (2010) 1603–1608.
[5] Z. Li, Z. Wu, K. Li, The high dispersion of DNA-multiwalled carbon nanotubes and their properties, Anal. Biochem. 387 (2009) 267–270.
[6] S.Y. Deng, G.Q. Jian, J.P. Lei, Z. Hu, H.X. Ju, A glucose biosensor based on direct electrochemistry of glucose oxidase immobilized on nitrogen-doped carbon nanotubes, Biosens. Bioelectron. 25 (2009) 373–377.
[7] G.S. Lai, F. Yan, H.X. Ju, Dual signal amplification of glucose oxidase-functionalized nanocomposites as a trace label for ultrasensitive simultaneous multiplexed electrochemical detection of tumor markers, Anal. Chem. 81 (2009) 9730–9736.
[8] A. Merkoci, M. Pumera, X. Llopis, B. Perez, M. del Valle, S. Alegret, New materials for electrochemical sensing VI: carbon nanotubes, Trends Anal. Chem. 24 (2005) 826–838.
[9] X. Yu, B. Munge, V. Patel, G. Jensen, A. Bhirde, J.D. Gong, S.N. Kim, J. Gillespie, J.S. Gutkind, F. Papadimitrakopoulos, J.F. Rusling, Carbon nanotube amplification strategies for highly sensitive immunodetection of cancer biomarkers, J. Am. Chem. Soc. 128 (2006) 11199–11205.
[10] X. Zeng, X. Li, X. Liu, Y. Liu, S. Luo, B. Kong, S. Yang, W. Wei, A third-generation hydrogen peroxide biosensor based on horseradish peroxidase immobilized on DNA functionalized carbon nanotubes, Biosens. Bioelectron. 25 (2009) 896–900.
[11] D. Baskaran, J.W. Mays, X.P. Zhang, M.S. Bratcher, Carbon nanotubes with covalently linked porphyrin antennae: photoinduced electron transfer, J. Am. Chem. Soc. 127 (2005) 6916–6917.
[12] W. Cheng, L. Ding, J. Lei, S. Ding, H.X. Ju, Effective cell capture with tetrapeptide-functionalized carbon nanotubes and dual signal amplification for cytosensing and evaluation of cell surface carbohydrate, Anal. Chem. 80 (2008) 3867–3872.
[13] H. Chen, F. Xi, X. Gao, Z. Chen, X. Lin, Bienzyme bionanomultilayer electrode for glucose biosensing based on functional carbon nanotubes and sugar–lectin biospecific interaction, Anal. Biochem. 403 (2010) 36–42.
[14] D.M. Guldi, G.M.A. Rahman, M. Prato, N. Jux, S.H. Qin, W. Ford, Single-wall carbon nanotubes as integrative building blocks for solar-energy conversion, Angew. Chem. Int. Ed. 44 (2005) 2015–2018.
[15] J. Wang, Y.H. Lin, Functionalized carbon nanotubes and nanofibers for biosensing applications, Trends Anal. Chem. 27 (2008) 619–626.
[16] W.W. Tu, J.P. Lei, H.X. Ju, Noncovalent nanoassembly of porphyrin on single-walled carbon nanotubes for electrocatalytic reduction of nitric oxide and oxygen, Electrochem. Commun. 10 (2008) 766–769.
[17] W. Cheng, L. Ding, S. Ding, Y. Yin, H.X. Ju, A simple electrochemical cytosensor array for dynamic analysis of carcinoma cell surface glycans, Angew. Chem. Int. Ed. 48 (2009) 6465–6468.
[18] B.E. Collins, J.C. Paulson, Cell surface biology mediated by low affinity multivalent protein–glycan interactions, Curr. Opin. Chem. Biol. 8 (2004) 617–625.
[19] R.S. Haltiwanger, J.B. Lowe, Role of glycosylation in development, Annu. Rev. Biochem. 73 (2004) 491–537.
[20] Y. Kinjo, D. Wu, G. Kim, G.W. Xing, M.A. Poles, D.D. Ho, M. Tsuji, K. Kawahara, C.H. Wong, M. Kronenberg, Recognition of bacterial glycosphingolipids by natural killer T cells, Nature 434 (2005) 520–525.
[21] P.M. Rudd, T. Elliott, P. Cresswell, I.A. Wilson, R.A. Dwek, Glycosylation and the immune system, Science 291 (2001) 2370–2376.
[22] B. Xia, C.L. Feasley, G.P. Sachdev, D.F. Smith, R.D. Cummings, Glycan reductive isotope labeling for quantitative glycomics, Anal. Biochem. 387 (2009) 162–170.
[23] M.M. Fuster, J.D. Esko, The sweet and sour of cancer: glycans as novel therapeutic targets, Nat. Rev. Cancer 5 (2005) 526–542.
[24] L. Ding, Q.J. Ji, R.C. Qian, W. Cheng, H.X. Ju, Lectin-based nanoprobes functionalized with enzyme for highly sensitive electrochemical monitoring of dynamic carbohydrate expression on living cells, Anal. Chem. 82 (2010) 1292–1298.
[25] J.A. Goetz, M.V. Novotny, Y. Mechref, Enzymatic/chemical release of *O*-glycans allowing MS analysis at high sensitivity, Anal. Chem. 81 (2009) 9546–9552.
[26] A. Kameyama, N. Kikuchi, S. Nakaya, H. Ito, T. Sato, T. Shikanai, Y. Takahashi, K. Takahashi, H. Narimatsu, A strategy for identification of oligosaccharide structures using observational multistage mass spectral library, Anal. Chem. 77 (2005) 4719–4725.
[27] X. Liu, D.J. McNally, H. Nothaft, C.M. Szymanski, J.R. Brisson, J. Li, Mass spectrometry-based glycomics strategy for exploring N-linked glycosylation in eukaryotes and bacteria, Anal. Chem. 78 (2006) 6081–6087.
[28] K. Hsu, K.T. Pilobello, L.K. Mahal, Analyzing the dynamic bacterial glycome with a lectin microarray approach, Nat. Chem. Biol. 2 (2006) 153–157.
[29] W. Huang, D. Wang, M. Yamada, L.X. Wang, Chemoenzymatic synthesis and lectin array characterization of a class of *N*-glycan clusters, J. Am. Chem. Soc. 131 (2009) 17963–17971.
[30] H. Tateno, N. Uchiyama, A. Kuno, A. Togayachi, T. Sato, H. Narimatsu, J. Hirabayashi, A novel strategy for mammalian cell surface glycome profiling using lectin microarray, Glycobiolgy 17 (2007) 1138–1146.
[31] L. Ding, W. Cheng, X.J. Wang, Y.D. Xue, J.P. Lei, Y.B. Yin, H.X. Ju, A label-free strategy for facile electrochemical analysis of dynamic glycan expression on living cells, Chem. Commun. (2009) 7161–7163.
[32] G. Entlichera, J.V. Koštířa, J. Kocoureka III, Studies on phytohemagglutinins isoelectric point and multiplicity of purified concanavalin A, Biochim. Biophys. Acta 236 (1971) 795–797.
[33] N. Srinivasan, S.M. Bane, S.D. Ahire, A.D. Ingle, R.D. Kalraiya, Poly *N*-acetyllactosamine substitutions on *N*- and not *O*-oligosaccharides or Thomsen-Friedenreich antigen facilitate lung specific metastasis of melanoma cells via galectin-3, Glycoconjugate J. 26 (2009) 445–456.
[34] S. Chen, T. Zheng, M.R. Shortreed, C. Alexander, L.M. Smith, Analysis of cell surface carbohydrate expression patterns in normal and tumorigenic human breast cell lines using lectin arrays, Anal. Chem. 79 (2007) 5698–5702.
[35] J.M. Nam, K.J. Jang, J.T. Groves, Detection of proteins using a colorimetric bio-barcode assay, Nat. Protoc. 2 (2007) 1438–1444.
[36] K.T. Pilobello, D.E. Slawek, L.K. Mahal, A ratiometric lectin microarray approach to analysis of the dynamic mammalian glycome, Proc. Natl. Acad. Sci. USA 104 (2007) 11534–11539.
[37] Z. Zhelev, H. Ohba, R. Bakalova, R. Jose, S. Fukuoka, T. Nagase, M. Ishikawa, Y. Baba, Fabrication of quantum dot–lectin conjugates as novel fluorescent probes for microscopic and flow cytometric identification of leukemia cells from normal lymphocytes, Chem. Commun. (2005) 1980–1982.
[38] Z.A. Liu, M. Jiang, J.H. Zhao, H.X. Ju, Circulating tumor cells in perioperative esophageal cancer patients: quantitative assay system and potential clinical utility, Clin. Cancer Res. 13 (2007) 2992–2997.
[39] T. Zheng, D. Peelen, L.M. Smith, Lectin arrays for profiling cell surface carbohydrate expression, J. Am. Chem. Soc. 127 (2005) 9982–9983.